

NBMLSS: probabilistic forecasting of electricity prices via Neural Basis Models for Location Scale and Shape

Alessandro Brusaferr^{a,*}, Danial Ramin^a, Andrea Ballarino^a

^a*CNR, Institute of Intelligent Industrial Technologies and Systems for Advanced Manufacturing, via A. Corti 12, Milan, Italy*

Abstract

Forecasters using flexible neural networks (NN) in multi-horizon distributional regression setups often struggle to gain detailed insights into the underlying mechanisms that lead to the predicted feature-conditioned distribution parameters. In this work, we deploy a Neural Basis Model for Location, Scale and Shape, that blends the principled interpretability of GAMLSS with a computationally scalable shared basis decomposition, combined by linear projections supporting dedicated stepwise and parameter-wise feature shape functions aggregations. Experiments have been conducted on multiple market regions, achieving probabilistic forecasting performance comparable to that of distributional neural networks, while providing more insights into the model behavior through the learned nonlinear feature level maps to the distribution parameters across the prediction steps.

Keywords: Neural Networks, GAMLSS, Time series, Electricity price, Forecasting, Day-ahead market

1. Introduction

Probabilistic forecasting of hourly electricity prices in day-ahead power markets (PEPF) is a complex problem with a significant impact. Accurate predictions and reliable uncertainty quantification are essential for a diverse array of

*Corresponding author

Email address: `alessandro.brusaferri@stiima.cnr.it` (Alessandro Brusaferrⁱ)

participants, including utilities, retailers, aggregators, and large consumers [1]. These enable informed decision-making in high-stakes scenarios such as trading strategies, resource scheduling, and optimal commitment by factoring in potential fluctuations and associated risks [2]. Moreover, electricity prices are characterized by high volatility and rapid changes driven by intricate factors, including distributed power demand, generation costs, and weather conditions [3]. The growing adoption of renewable energy sources, vital for mitigating global emissions, introduces additional complexities to this landscape [4]. Furthermore, fluctuations in gas prices critically affect power plant operations and overall electricity pricing.

A wide range of methods has been proposed over the past decades to characterize the inherent uncertainty in probabilistic forecasts of electricity prices, including simple prediction intervals, discrete conditional quantiles, and full distributional estimation [5]. We refer interested readers to recent reviews for a detailed treatment [6],[7]. Nowadays, an increasing research interest can be observed in neural network-based approaches, leveraging their flexible mapping capabilities in the conditioning space and exploiting the increasingly available computational power and tools [7]. In this context, Distributional neural networks (DDNN) parameterizing flexible forms, such as the Johnson’s SU, have been recently shown to provide a valuable support in characterizing the complex patterns exhibited by the target price distributions, including, e.g., sensible heteroskedasticity, fat tails and skewness [8]. However, these enhanced capabilities come with a limited degree of interpretability. The inherent black-box nature of these models restricts the ability to understand how specific forecasts are generated, which may hinder their adoption in high-risk environments. Crucially, the way in which these models shape output density parameters based on input features throughout the prediction horizon remains opaque to users.

Post-hoc model-agnostic techniques such as LIME surrogate models and Shapley values extensions have been proposed to provide a certain degree of explainability through local approximations and feature importance [9]. Still, faithful global explanations of the complex latent computations performed by

the original models are difficult to achieve [10]. Hence, a distinct line of research studies aims to enhance transparency in neural networks by acting directly on the architecture. A representative class of approaches in this field is the Neural Additive Model (NAM) introduced by [11]. Following the well-known Generalized Additive Models (GAM) framework, NAMs leverage a linear combination of flexible neural networks, each attending to single features, thus elucidating the actual relationships to the outputs. Recently, authors in [12] have extended NAMs from the original point prediction to a broader distributional regression setup, leading to Neural Additive Models for Location, Scale, and Shape (NAMLSS). By iterating on the general class of GAMLSS [13], as NAMs do on GAMs, NAMLSSs aim to reveal the specific effects of input features on the shapes of complex response distributions beyond the mean, including variance, skewness, and tailedness. To this end, NAMLSS leverages a specific neural network for each input feature or even for each distribution parameter when configured to resemble the GAMLSS form. Despite their flexible and interpretable feature-level representation capabilities, such NAMLSS designs suffer from expansive computational scaling under increasing conditioning space and multi-horizon setups, making them impractical for the target PEPF applications at hand. To the best of our knowledge, studies exploring extensions to the NAMLSS concept for addressing challenging probabilistic time series forecasting applications such as PEPF are still lacking in the literature.

Following the aforementioned developments and moving from reported open issues, the major scope of the present work is to contribute to the investigation of the general Neural Additive Model framework within the PEPF field. In particular, we aim to assess whether more interpretable architectural forms can reach the state of the art distributional neural networks (DDNNs) under consistent parameterizations. To this end, we extend the NAMLSS model by leveraging a basis decomposition of the feature shape functions [14]. Specifically, a unique neural network is exploited to learn a set of basis functions shared across all features in a multi-task setup, which are then combined by linear projections supporting dedicated stepwise and parameter-wise shape functions

aggregations. The whole model is trained end-to-end through backpropagation, following the multi-horizon time series framework commonly adopted in DDNNs. We label the developed model NBMLSS hereafter, standing for Neural Basis Model for Location, Scale and Shape. The experiments were conducted using open datasets [15] from multiple day-ahead markets with heterogeneous characteristics.

2. Methods

As introduced in the previous section, this work is dedicated to the class of multi-step PEPF systems designed to learn the target price distributions over the different steps of the day-ahead horizon. H represents the length of the target prediction horizon $\mathbf{y}_d = [y_{d,1}, \dots, y_{d,H}]$ in each d -th day, e.g., next 24 hours. We concentrate on the feed-forward class (i.e., DNN) to align with the architecture of the original distributional neural network proposed in [8] for PEPF. The conditioning set is then structured as a flattened tensor $\mathbf{x}_d = [x_{d,1}, \dots, x_{d,n_f}]$ of size n_f typically involving the past values of the target price, the available dynamic covariates (e.g., generation and load forecasts) as well as constant features (e.g., day-of-week encoding, etc). We leave to future extensions the investigation of alternative architectural designs, such as hour-specific and recursive approaches. Considering a dense feed-forward map with two hidden layers to shorten notation, the NBMLSS model architecture (depicted in Figure 1) is formally defined as follows:

$$z_k(x_{d,i}) = \mathbf{a} \left[\sum_{j=1}^{n_u} \omega_{j,k}^{(2)} \mathbf{a} \left[\omega_j^{(1)} x_{d,i} \right] + \omega_{0,k}^{(2)} \right], k = 1, \dots, n_z \quad (1)$$

$$f_i(x_{d,i}) = \sum_{k=1}^{n_z} w_{i,k} z_k(x_{d,i}), i = 1, \dots, n_f \quad (2)$$

$$\theta_h^p(\mathbf{x}_d) = \mathbf{g}^p \left[\beta_h^p + \sum_{i=1}^{n_f} v_{h,i}^p f_i(x_{d,i}) \right], h = 1, \dots, H; p = 1, \dots, n_p \quad (3)$$

The first equation represents the k -th shared basis function [14] in the set of size $n_z \in \mathbb{Z}^+$. The second and third equations structure the stepwise target

conditional distribution parameters $p = [1, \dots, n_p]$ as trainable linear projections from the basis output $z_k(x_{d,i})$ computed for each feature $x_{d,i}$. In particular, $w_{i,k} \in \mathbb{R}^{n_f \times n_z}$ is aimed to aggregate the shared basis into feature specific shape functions $f_i(\cdot)$, $v_{h,i}^p \in \mathbb{R}^{H \times n_f}$ combines the shape functions outputs into the stage-wise distribution parameterization, and $\beta_h^p \in \mathbb{R}$ trainable biases. In the shared network Equation 1, $\omega_j^{(1)} \in \mathbb{R}^{n_u}$ and $\omega_{j,k}^{(2)} \in \mathbb{R}^{n_u \times n_z}$ depict the trainable weights for the first and second hidden layer respectively, whereas $\mathbf{a}[\cdot]$ repre-

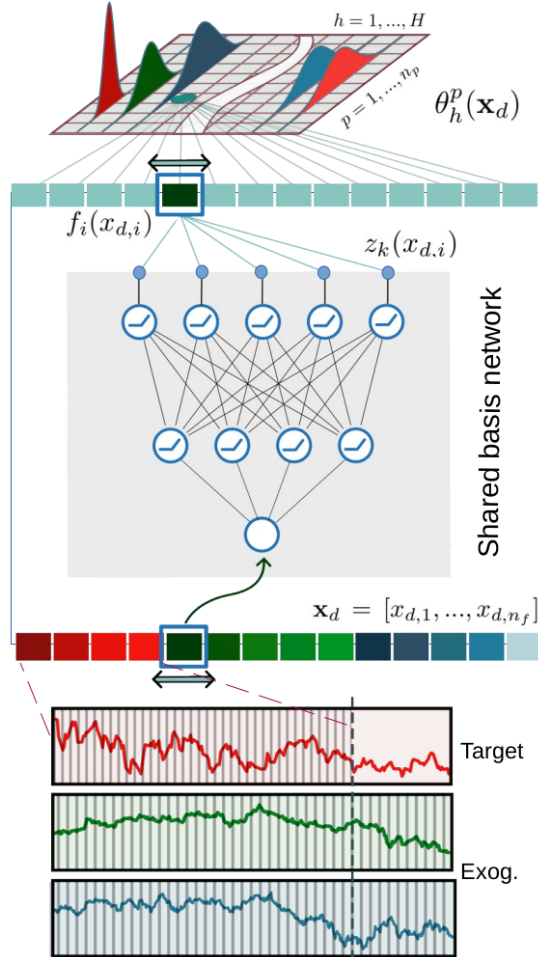


Figure 1: NBMLSS schema

sents the nonlinear activation functions. Although the vanilla NAM exploits exponential units activation to identify jagged maps [11], subsequent studies have reported that standard ReLU provides a better alternative in practice [16]. Dropout layers are also included on top of both hidden layers to foster basis decorrelation by random removal [11]. $\mathbf{g}^p[\cdot]$ resembles the link function of the p -th parameter, designed depending on the adopted density form [12]. For instance, considering the Johnson’s SU density:

$$d^h(\chi; \mathbf{x}_d) = \frac{\tau_d^h}{\sigma_d^h \sqrt{2\pi}} \frac{1}{\sqrt{1 + \left(\frac{\chi - \lambda_d^h}{\sigma_d^h}\right)^2}} e^{-\frac{1}{2} \left[\zeta_d^h + \tau_d^h \sinh^{-1} \left(\frac{\chi - \lambda_d^h}{\sigma_d^h} \right) \right]^2} \quad (4)$$

the link functions are computed as:

$$\Theta(\mathbf{x}_d) = [\theta_1^1(\mathbf{x}_d), \dots, \theta_H^1(\mathbf{x}_d), \dots, \theta_1^{n_p}(\mathbf{x}_d), \dots, \theta_H^{n_p}(\mathbf{x}_d)] \quad (5)$$

$$\lambda_d^h = \Theta(\mathbf{x}_d)^{[h]} \quad (6)$$

$$\sigma_d^h = \epsilon + \gamma \text{Softplus} \left(\Theta(\mathbf{x}_d)^{[H+h]} \right) \quad (7)$$

$$\tau_d^h = 1 + \gamma \text{Softplus} \left(\Theta(\mathbf{x}_d)^{[2 \cdot H+h]} \right) \quad (8)$$

$$\zeta_d^h = \Theta(\mathbf{x}_d)^{[3 \cdot H+h]} \quad (9)$$

$$\text{Softplus}(x) = \log(1 + e^x) \quad (10)$$

where $\lambda_d^h, \sigma_d^h, \tau_d^h, \zeta_d^h$ are the density location, scale, tailweight and skewness conditioned on the input features x_d . $\epsilon = 1e^{-3}$ and $\gamma = 3$ are correction factors commonly introduced for computational purposes. Similar transformations can be directly derived for further density parameterization, such as ensuring that standard deviation and degrees of freedom remain positive in the Student-t distributions. The whole model is trained by backpropagation following a dynamic recalibration process, using the the negative log-likelihood computed on the output distribution as loss function. The samples $\mathcal{D}_n \equiv \{(x_d, y_d)\}_{d=1}^n$ are derived by applying standard moving window techniques on both conditioned/exogenous time series followed by concatenation. An early stopping procedure with patience is included by leveraging a validation subset. Additional details are provided in the next section, devoted to the experiment setup.

A further open issue in PEPF concerns the critical distribution shifts observed in recent power markets settlements. While models recalibration has been shown to provide partial mitigations, several research studies in the time series domain have reported reductions in point prediction errors by integrating Reversible Instance normalization (RevIN) layers [17]. However, whether RevIN can provide valuable support to NN based PEPF systems beyond conventional dataset-level standardization techniques remains an open question requiring further investigation. Consequently, we deploy RevIN within both NBMLSS and state of the art distributional NN architectures by introducing bijector layers aimed at reshaping the parameterized distributions back to the original scale.

3. Experiments and results

To evaluate the proposed approach, we leverage the open dataset recently structured by [15], integrating data from the ENTSO-E transparency platform across several European markets. Moreover, this dataset includes recent time periods to enable the assessment of models performance under the increasing volatility levels faced by forecasters nowadays. In particular, we focus on the day-ahead prices of Germany, Spain, Belgium, and Sweden-Stockholm (SE3) covering heterogeneous conditions. The investigation of further datasets is left for future work.

All datasets include hourly load and wind/solar generation predictions as exogenous features. Besides, the temporal age feature and day-of-the-week indicator have been included, encoded in cyclical sine-cosine form. As introduced above, the input/output samples are built from the time series by means of a standard moving window technique. For the scope of the present study, the conditioning vectors x_d have been structured by integrating the price values over the previous days $d-1$, $d-2$, $d-7$ alongside the day-ahead exogenous variables, totaling $n_f=147$ features.

For each region, the out-of-sample test set covers the last year of available observations, starting from 2022/07/01 to 2023/6/30. The training/validation

Table 1: Hyperparameters selected by the grid-search procedure for each zone

N-DNN	BE	DE	ES	SE
n_u	640	768	640	512
l_r	5e-4	1e-4	1e-4	1e-3
d_r	0.3	0.3	0.3	0.1
J-DNN	BE	DE	ES	SE
n_u	640	768	768	640
l_r	5e-5	1e-4	5e-5	5e-5
d_r	0.1	0.3	0.3	0.3
J-NBMLSS	BE	DE	ES	SE
n_u	64	128	32	128
l_r	5e-4	5e-4	5e-4	5e-4
d_r	0.5	0.5	0.3	0.5

subsets involve samples from 2019/1/1 up to the first test date. Following [7], we have used one year of data prior to the start of the test set for hyperparameter tuning through cross-validation (via Optuna [18]), while a random subsplit of 20% has been adopted for early stopping.

To balance the computational costs of updating the models under changing conditions across different experimental configurations, we employed weekly recalibration on the test set and retraining using four sequential folds during cross-validation. Training is performed by means of Adam - minimizing the negative log likelihood loss (NLL) - with a maximum number of 800 epochs and a patience of 20 epochs. The batch size has been set to 128.

Considering the analysis performed in previous studies (see e.g., [19],[8]), the Distributional Neural Networks (DDNNs) have been structured with two hidden layers, including ReLU activations and dropout regularization. Both Normal (N) and JSU (J) density parameterization are investigated. The number of units in each layer, the Dropout rate, as well as the learning rate have been tuned by grid search in the discrete sets [128, 512, 640, 768], [0, 0.1, 0.3, 0.5] and [1e-3,

5e-4, 1e-4, 5e-5] respectively. For NBMLSS, the number of units in the shared feature network has been searched within a reduced range $n_u, n_z=[32, 64, 128, 256]$, as we observed that the procedure selected smaller values during the initial experiments on the datasets. Both models have been implemented using the TensorFlow Probability library [20]. Table 1 reports the tuned configurations for each market.

Following [8], we have implemented both DDNN and NBMLSS within ensembles, aggregated either through uniform mixture (i.e., probability distribution aggregation - labeled 'p') and quantile averaging (i.e., vincentization - labeled 'v'). To this end, each model configuration has been recalibrated multiple times (i.e., 5), starting from different random initializations. The predicted distribution quantiles are estimated by generating 10000 samples for each test item. Post-hoc sorting is employed to fix potential quantile crossing.

The probabilistic forecasting performances obtained on the test sets are reported in Tables 2-5, where the suffix 'r' represents the backbone model including the RevIn layer, while 's' stands for the conventional Z-score normalization fitted on the training samples (see, e.g., [19]) The Continuous Ranked Probability Score (CRPS) has been approximated by the average Pinball loss across 99 percentiles. We report the Kupiec test results for unconditional coverage (with significance level 0.05) on 50% and 90% prediction intervals beside the quantitative coverage probability (PICP), while the overall coverage achieved across the percentiles is depicted in the Figures 2-5. Moreover, we show in Figure 6 the results of the multivariate Diebold and Mariano (DM) test on the differences in the CRPS loss norms between the models predictions.

First, it can be noted that the JSU parameterization has led to better performances than the Normal form. This is in line with the observations reported in the previous studies on DDNNs, motivated by its greater flexibility in mapping complex aleatoric uncertainty patterns.

Secondly, NBMLSS has achieved CRPS results that are comparable to, and in some cases better than, those of the DDNN under consistent settings (e.g., on BE with RevIN/standard normalization).

Table 2: BE - Test set results

	PICP _{50%} (Kupiec)	PICP _{90%} (Kupiec)	PICP _{98%} (Kupiec)	MAE	CRPS
N-DNN _{s,v}	58.0(6)	93.2(12)	97.7(22)	32.443	11.819
N-DNN _{s,p}	58.4(4)	94.1(8)	98.2(22)	32.275	11.805
N-DNN _{r,v}	58.3(2)	91.2(20)	97.1(20)	26.184	9.704
N-DNN _{r,p}	58.7(2)	91.9(15)	97.6(20)	26.206	9.709
J-DNN _{s,v}	50.3(20)	89.7(18)	96.9(16)	29.628	10.714
J-DNN _{s,p}	51.6(18)	90.8(19)	97.5(21)	29.691	10.726
J-DNN _{r,v}	51.4(20)	88.9(21)	96.6(17)	26.213	9.535
J-DNN _{r,p}	52.2(19)	89.7(23)	97.1(20)	26.211	9.534
J-NBMLSS _{s,v}	53.6(16)	90.3(21)	97.4(20)	28.242	10.349
J-NBMLSS _{s,p}	53.7(16)	90.7(21)	97.7(21)	28.189	10.338
J-NBMLSS _{r,v}	49.9(24)	87.8(19)	96.5(14)	25.350	9.284
J-NBMLSS _{r,p}	50.1(24)	88.3(21)	96.8(18)	25.362	9.282

Table 3: DE - Test set results

	PICP _{50%} (Kupiec)	PICP _{90%} (Kupiec)	PICP _{98%} (Kupiec)	MAE	CRPS
N-DNN _{s,v}	59.9(0)	93.7(11)	97.8(17)	33.022	11.968
N-DNN _{s,p}	60.1(1)	94.2(9)	98.1(17)	32.969	11.960
N-DNN _{r,v}	54.2(12)	89.7(15)	96.2(14)	24.863	9.094
N-DNN _{r,p}	54.8(12)	90.5(15)	96.8(18)	24.860	9.093
J-DNN _{s,v}	47.5(19)	87.2(14)	95.6(8)	25.872	9.386
J-DNN _{s,p}	48.9(21)	88.7(17)	96.3(10)	25.940	9.393
J-DNN _{r,v}	47.9(17)	87.1(15)	95.6(9)	25.350	9.223
J-DNN _{r,p}	49.0(19)	88.1(14)	96.3(13)	25.347	9.212
J-NBMLSS _{s,v}	53.2(18)	90.2(17)	97.0(17)	24.708	9.019
J-NBMLSS _{s,p}	53.7(18)	90.8(18)	97.4(20)	24.649	9.005
J-NBMLSS _{r,v}	46.5(17)	86.3(13)	96.2(12)	24.331	8.834
J-NBMLSS _{r,p}	46.8(16)	86.9(14)	96.7(16)	24.333	8.830

Table 4: ES - Test set results

	PICP _{50%} (Kupiec)	PICP _{90%} (Kupiec)	PICP _{98%} (Kupiec)	MAE	CRPS
N-DNN _{s,v}	52.3(18)	87.6(17)	94.7(3)	16.788	6.207
N-DNN _{s,p}	53.3(17)	88.8(19)	95.6(8)	16.766	6.196
N-DNN _{r,v}	55.9(10)	89.4(21)	95.6(5)	16.211	5.996
N-DNN _{r,p}	56.3(9)	89.9(22)	96.2(13)	16.205	5.995
J-DNN _{s,v}	47.1(19)	83.2(2)	92.9(0)	16.454	6.139
J-DNN _{s,p}	48.4(21)	84.7(3)	93.8(0)	16.466	6.126
J-DNN _{r,v}	49.1(20)	86.9(14)	95.3(5)	16.489	6.044
J-DNN _{r,p}	49.8(20)	87.6(17)	95.9(7)	16.476	6.038
J-NBMLSS _{s,v}	48.0(22)	83.4(3)	92.6(0)	16.675	6.239
J-NBMLSS _{s,p}	48.3(23)	84.2(4)	93.6(0)	16.678	6.233
J-NBMLSS _{r,v}	49.7(24)	87.9(16)	95.5(6)	16.308	5.965
J-NBMLSS _{r,p}	50.2(24)	88.2(21)	96.0(8)	16.302	5.962

Table 5: SE - Test set results

	PICP _{50%} (Kupiec)	PICP _{90%} (Kupiec)	PICP _{98%} (Kupiec)	MAE	CRPS
N-DNN _{s,v}	54.7(14)	89.6(15)	94.8(7)	41.726	15.794
N-DNN _{s,p}	54.2(15)	90.5(18)	95.5(7)	41.469	15.606
N-DNN _{r,v}	56.9(9)	89.5(24)	96.1(12)	34.506	12.813
N-DNN _{r,p}	57.2(7)	90.5(22)	96.8(19)	34.377	12.797
J-DNN _{s,v}	43.9(10)	83.1(5)	92.9(1)	39.040	14.529
J-DNN _{s,p}	44.5(12)	84.2(5)	94.0(3)	39.262	14.527
J-DNN _{r,v}	48.9(13)	85.3(7)	94.6(1)	33.498	12.261
J-DNN _{r,p}	49.7(14)	86.1(9)	95.2(7)	33.494	12.258
J-NBMLSS _{s,v}	47.9(22)	86.1(7)	94.3(0)	34.848	13.063
J-NBMLSS _{s,p}	47.9(21)	86.5(9)	94.7(0)	34.423	12.949
J-NBMLSS _{r,v}	45.7(14)	85.0(1)	94.6(0)	32.637	11.999
J-NBMLSS _{r,p}	46.0(15)	85.5(3)	95.2(4)	32.606	11.987

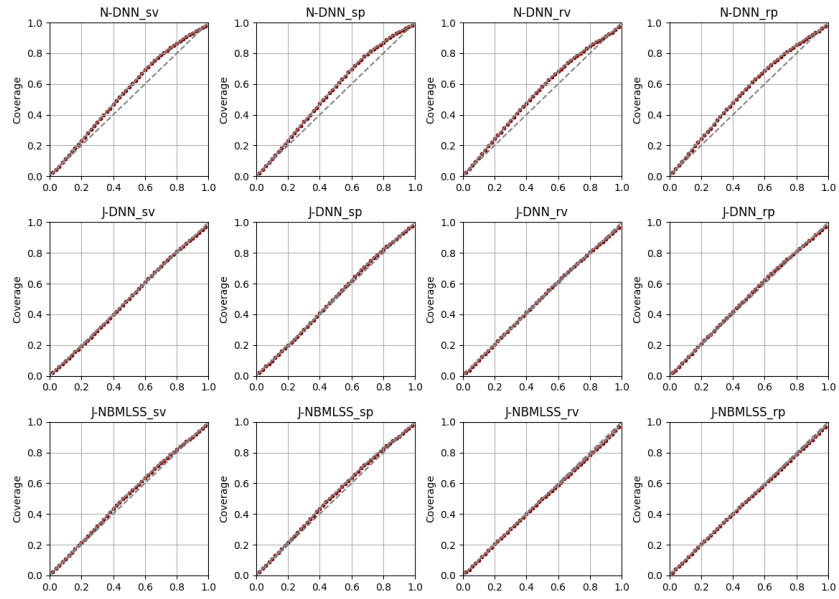


Figure 2: Calibration plots - BE test set

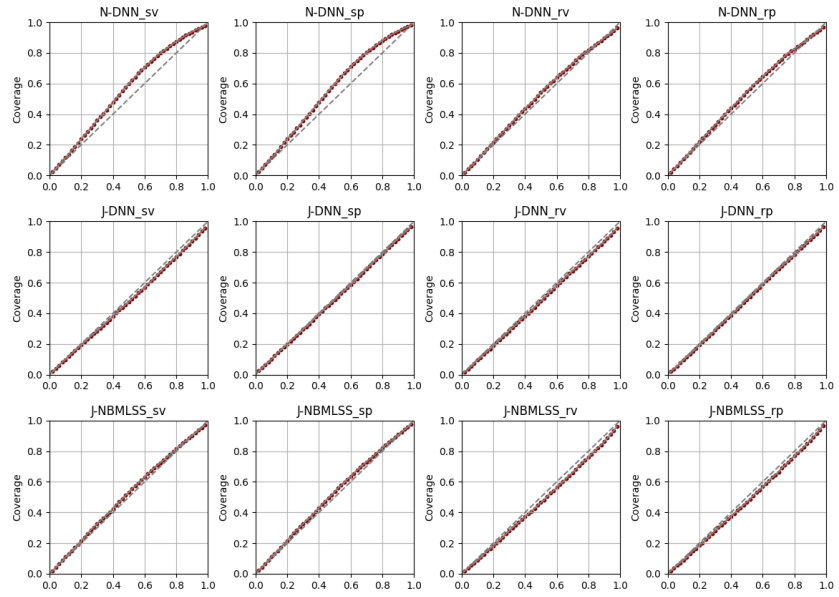


Figure 3: Calibration plots - DE test set

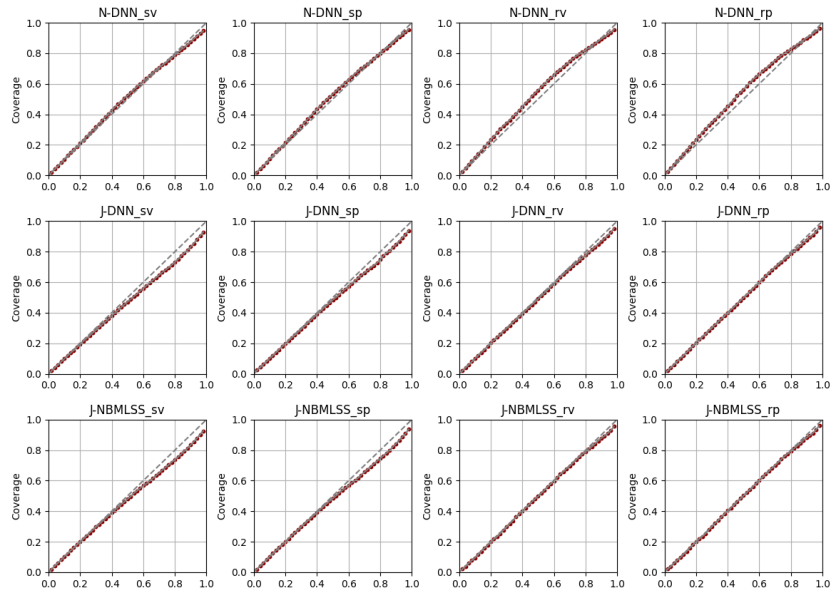


Figure 4: Calibration plots - ES test set

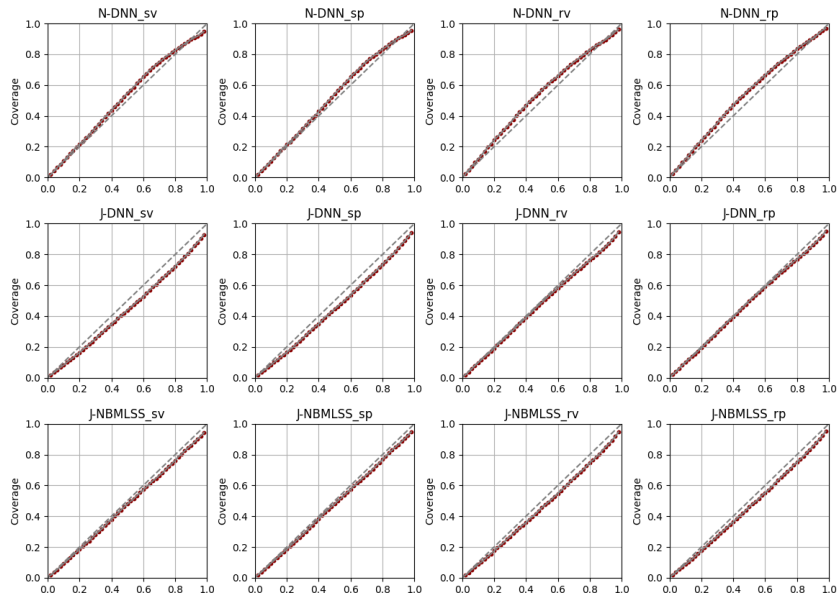


Figure 5: Calibration plots - SE test set

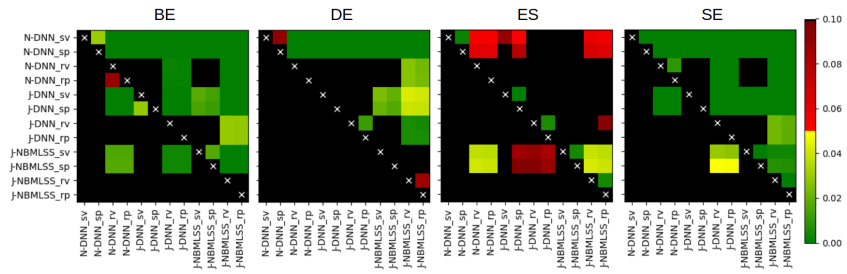


Figure 6: DM test on test set CRPS scores

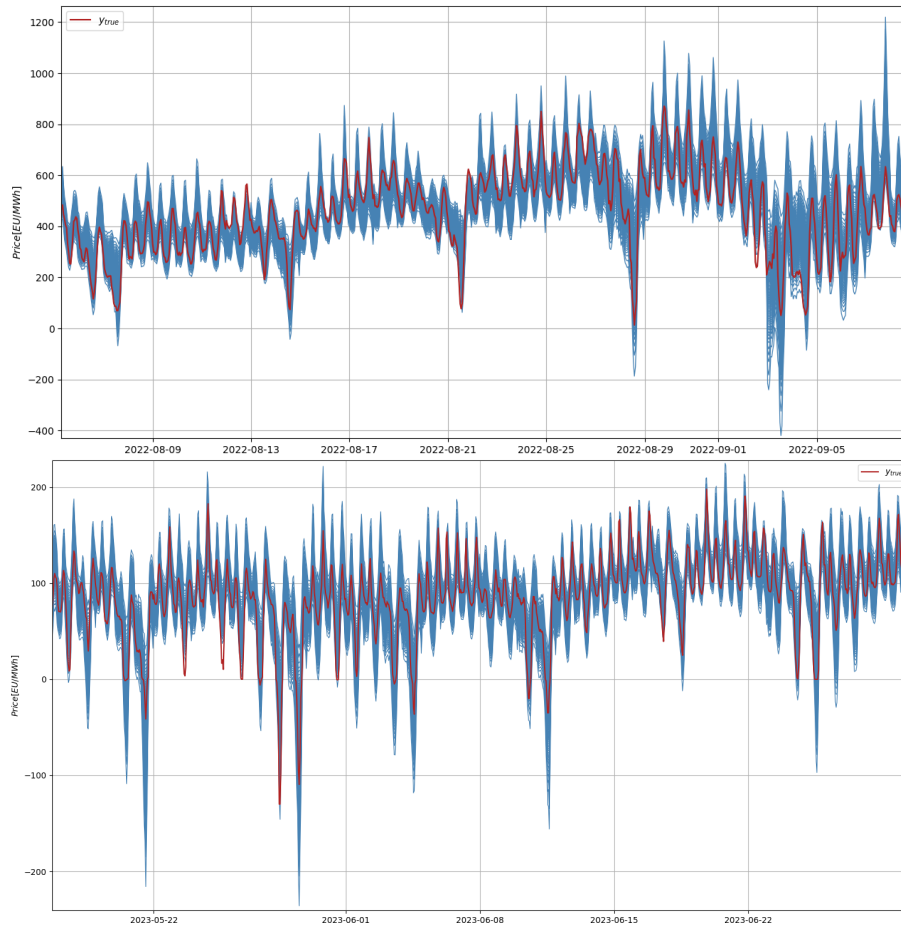


Figure 7: Samples of predicted distribution percentiles on DE market

Across the different regions, the introduction of the RevIN layer appears to lead to lower CRPS values on average, beyond lower Mean Absolute Errors (on the extracted 0.5 quantile).

Still, RevIN provides only partial mitigation, beyond the conventional dynamic recalibration, for strong drifts such as the one that affected most European power markets in 2022 following the Ukrainian conflict. Indeed, both N-DNN and J-DNN show excessively tails spikes in several stages during this period (see e.g., the negative spike around -400 euro/MWh in the upper part of Figure 7, reporting samples of the DE price in 2022). Similar problems with distributional neural networks in addressing sensible shifts have been reported in recent works [21]. J-NBMLSS also appears to be critically affected, presumably because it is based on a restricted feature-wise mapping of the same network parameterization. The local normalization performed by RevIN is involved in such process, since shifting and centering observations sample-wise. Although the predicted distributions show better matches to the actual price settlements once the market dynamics return to more stable conditions (e.g., the lower part of Figure 7, reporting samples of the DE price in 2023), this issue warrants further investigation, e.g., by integrating alternative transformations, specific conditioning features, etc.

Moreover, we observe in Tables 2-5 that both J-DNN and J-NBMLSS tend to produce partially overconfident probabilistic forecasts in multiple cases, reflecting an open problem in neural network-based techniques [22], [23]. The quantile averaging shows lower PICP values than the probability aggregation alternative, due to its typical ability to provide sharper forecasts [24]. The specific impact on target coverage depends on the actual dispersion of the underlying ensemble components (see e.g., DE vs ES). To address these issues, we plan to integrate ex-post conformal inference-based techniques in future extensions of this work.

Beyond the probabilistic forecasting performance achieved, the main aim of the NBMLSS architecture is to provide users with a representation of the relationships identified between each input feature and the target distribution parameters over the horizon, thereby revealing the underlying mechanisms driv-

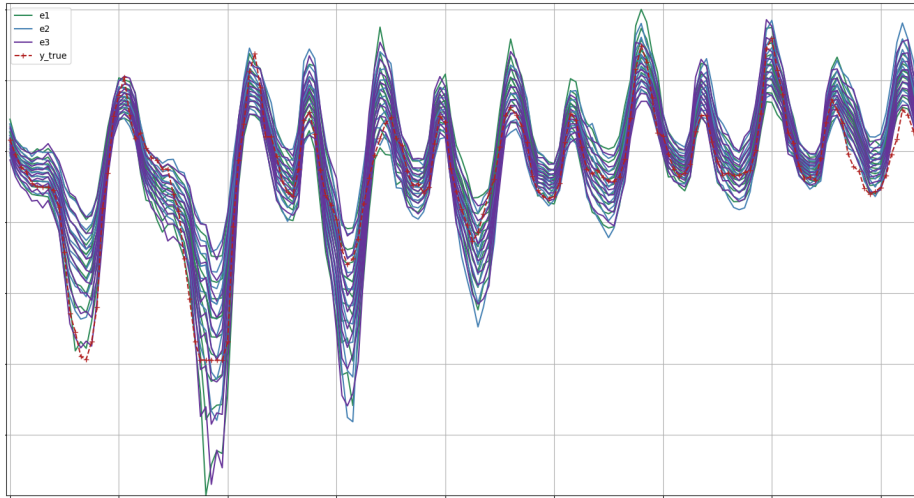


Figure 8: Samples of predicted distribution deciles on DE market of 3 ensemble components

ing to the output predictions. Figures 9-10 report samples of extracted shape functions, during three random recalibration runs (i.e., ensemble components) over the last test samples, while Figure 8 depicts the predicted deciles to support better legibility. Interestingly, it can be observed that while the predicted distributions assume similar patterns, these are constructed by quite heterogeneous shape functions combinations. Such latent behavior in neural additive models has also been reported in other recent studies showing the relation to the concavity among the features (see e.g., [25],[26] and references therein). Although concavity regularizers have been proposed to enforce decorrelation, nonlinear dependencies of shape functions have not yet been addressed in the literature, and the integration of additional penalties remains a compelling area for future research [26]. Still, we concur with the authors in [26] that optimal feature selection should be conducted by domain experts, and that offering an ensemble of solutions, rather than a single candidate, currently appears to be the most practical trade-off. This is particularly critical in time series applications, where redundancy in the conditioning set is more common than exceptional (as can occur, for example, among price values during early morning hours on closed

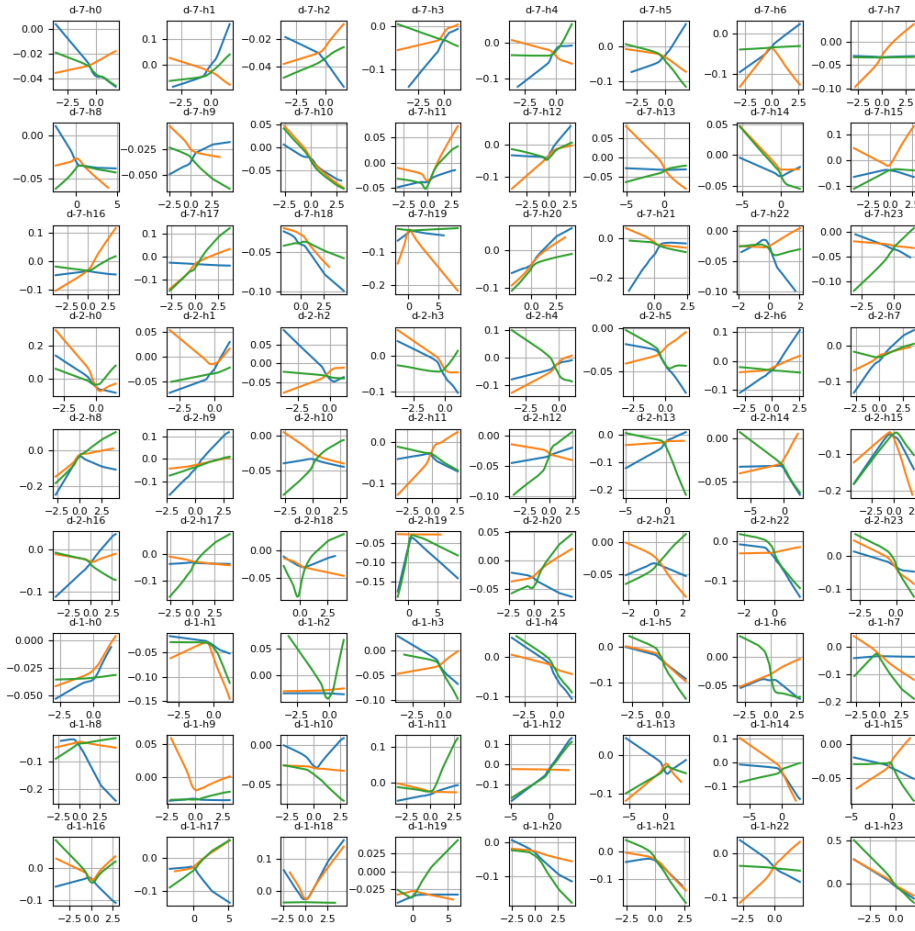


Figure 9: Shape functions of 3 ensemble components on past price features (DE-h8-loc)

days). In this context, neural additive models such as NBMLSS can complement the flexibility of DDNN (e.g., through hybrid ensembles) by offering deeper insights into the underlying feature’s contribution across the domain, thereby supporting users during the critical phases of model design.

4. Conclusions and next developments

In this work, we have tackled probabilistic electricity price forecasting through Neural Basis Models for Location Scale and Shape, with the aim of assessing

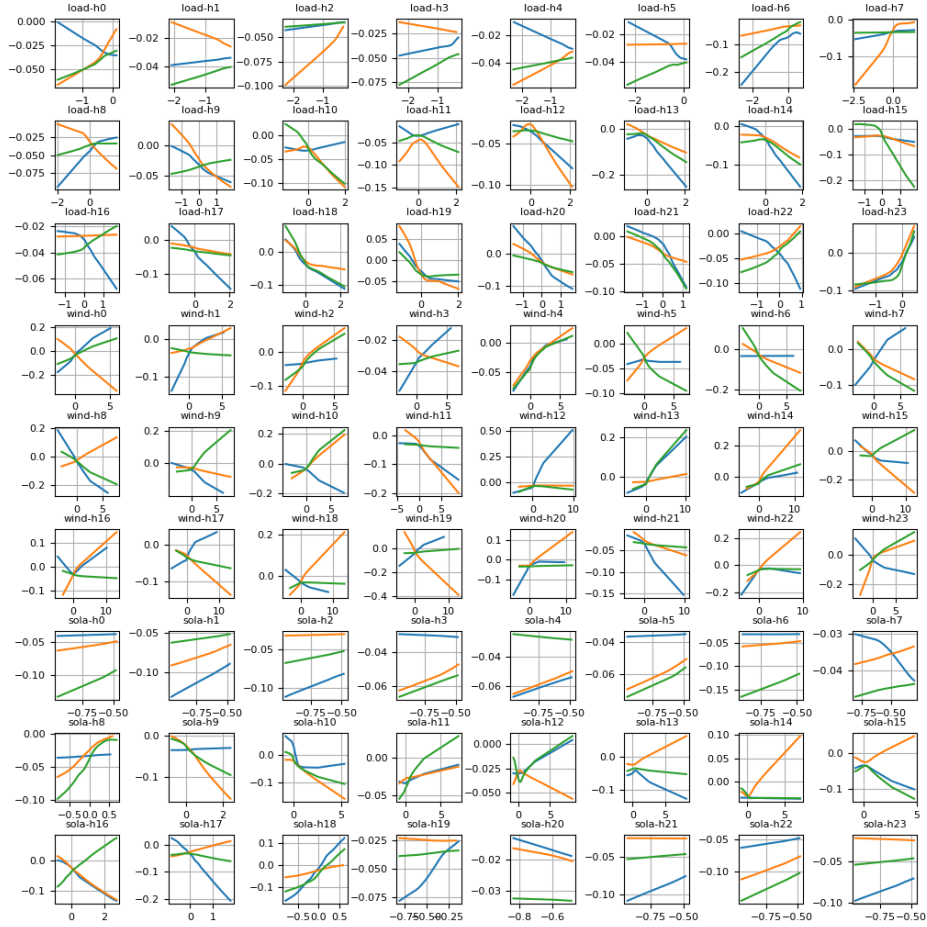


Figure 10: Shape functions of 3 ensemble components on exogenous features (DE-h8-loc)

whether these more interpretable architectural forms can reach the state-of-the-art distributional neural networks (DDNNs). To enhance computational scalability under increasing conditioning space and multi-horizon setups, we have exploited a unique dense map aimed at learning a set of share basis combined by trainable linear projections into the stage-wise distribution parameterization. Experiments have been conducted on open datasets from diverse power markets, incorporating recent time periods to support assessments under the increasing volatility levels that forecasters are facing. The proposed approach

has achieved scores comparable, and in some cases improved, relative to those of the DDNN under consistent settings, while the Johnson’s SU obtained better performance than the conventional Normal form. This can be due to its greater flexibility in mapping complex aleatoric uncertainty patterns. Next, we have inspected samples of feature shape functions extracted by the model under different random initializations, pointing to the challenging concavity problem. Still, we envision several avenues of future research, including the investigation of second-order interactions, the integration of eXplainable AI techniques (e.g., SHAP), further transformations as well as different components to better handle nonlinear dependencies within the conditioning sets. Moreover, we plan to investigate different probabilistic forecasting tasks, over both short and long term horizons, and network architectures.

References

- [1] A. Mashlakov, T. Kuronen, L. Lensu, A. Kaarna, S. Honkapuro, Assessing the performance of deep learning models for multivariate probabilistic energy forecasting, *Applied Energy* 285 (2021) 116405. doi:<https://doi.org/10.1016/j.apenergy.2020.116405>.
URL <https://www.sciencedirect.com/science/article/pii/S0306261920317748>

- [2] A. Wagner, E. Ramentol, F. Schirra, H. Michaeli, Short- and long-term forecasting of electricity prices using embedding of calendar information in neural networks, *Journal of Commodity Markets* (2022) 100246doi:<https://doi.org/10.1016/j.jcomm.2022.100246>.
URL <https://www.sciencedirect.com/science/article/pii/S2405851322000046>

- [3] A. Ciarreta, B. Martinez, S. Nasirov, Forecasting electricity prices using bid data, *International Journal of Forecasting* (2022). doi:<https://doi.org/10.1016/j.ijforecast.2022.05.011>.

URL <https://www.sciencedirect.com/science/article/pii/S0169207022000711>

- [4] S. Madadkhani, S. Ikonnikova, Toward high-resolution projection of electricity prices: A machine learning approach to quantifying the effects of high fuel and co2 prices, *Energy Economics* 129 (2024) 107241. doi:<https://doi.org/10.1016/j.eneco.2023.107241>.

URL <https://www.sciencedirect.com/science/article/pii/S0140988323007399>

- [5] A. Brusaferrri, M. Matteucci, P. Portolani, A. Vitali, Bayesian deep learning based method for probabilistic forecast of day-ahead electricity prices, *Applied Energy* 250 (2019) 1158–1175. doi:<https://doi.org/10.1016/j.apenergy.2019.05.068>.

URL <https://www.sciencedirect.com/science/article/pii/S0306261919309237>

- [6] J. Nowotarski, R. Weron, Recent advances in electricity price forecasting: A review of probabilistic forecasting, *Renewable and Sustainable Energy Reviews* 81 (2018) 1548–1568. doi:<https://doi.org/10.1016/j.rser.2017.05.234>.

URL <https://www.sciencedirect.com/science/article/pii/S1364032117308808>

- [7] J. Lago, G. Marcjasz, B. De Schutter, R. Weron, Forecasting day-ahead electricity prices: A review of state-of-the-art algorithms, best practices and an open-access benchmark, *Applied Energy* 293 (2021) 116983. doi:<https://doi.org/10.1016/j.apenergy.2021.116983>.

URL <https://www.sciencedirect.com/science/article/pii/S0306261921004529>

- [8] G. Marcjasz, M. Narajewski, R. Weron, F. Nov, Distributional neural networks for electricity price forecasting, *Energy Economics* 125 (2023) 106843. doi:<https://doi.org/10.1016/j.eneco.2023.106843>.

URL <https://www.sciencedirect.com/science/article/pii/S0140988323003419>

- [9] L. Tschora, E. Pierre, M. Plantevit, C. Robardet, Electricity price forecasting on the day-ahead market using machine learning, *Applied Energy* 313 (2022) 118752. doi:<https://doi.org/10.1016/j.apenergy.2022.118752>.

URL <https://www.sciencedirect.com/science/article/pii/S0306261922002057>

- [10] C. Rudin, Stop explaining black box machine learning models for high stakes decisions and use interpretable models instead, *Nature Machine Intelligence* 1 (2019) 206–215. doi:[10.1038/s42256-019-0048-x](https://doi.org/10.1038/s42256-019-0048-x).

- [11] R. Agarwal, L. Melnick, N. Frosst, X. Zhang, B. Lengerich, R. Caruana, G. E. Hinton, Neural additive models: interpretable machine learning with neural nets, in: *Proceedings of the 35th International Conference on Neural Information Processing Systems, NIPS '21*, Curran Associates Inc., Red Hook, NY, USA, 2024.

- [12] A. Thielmann, R.-M. Kruse, T. Kneib, B. Säfken, Neural additive models for location scale and shape: A framework for interpretable neural regression beyond the mean, in: S. Dasgupta, S. Mandt, Y. Li (Eds.), *Proceedings of The 27th International Conference on Artificial Intelligence and Statistics*, Vol. 238 of *Proceedings of Machine Learning Research*, PMLR, 2024, pp. 1783–1791.

URL <https://proceedings.mlr.press/v238/frederik-thielmann24a.html>

- [13] S. Hirsch, J. Berrisch, F. Ziel, Online distributional regression (2024). [arXiv:2407.08750](https://arxiv.org/abs/2407.08750).

URL <https://arxiv.org/abs/2407.08750>

- [14] F. Radenovic, A. Dubey, D. Mahajan, Neural basis models for interpretability, in: *Proceedings of the 36th International Conference on Neural Infor-*

mation Processing Systems, NIPS '22, Curran Associates Inc., Red Hook, NY, USA, 2024.

- [15] K. Aliyon, J. Ritvanen, Deep learning-based electricity price forecasting: Findings on price predictability and european electricity markets, *Energy* 308 (2024) 132877. doi:<https://doi.org/10.1016/j.energy.2024.132877>.
URL <https://www.sciencedirect.com/science/article/pii/S0360544224026513>
- [16] K. Bouchiat, A. Immer, H. Yèche, G. Rätsch, V. Fortuin, Improving neural additive models with bayesian principles (2024). arXiv:2305.16905.
URL <https://arxiv.org/abs/2305.16905>
- [17] T. Kim, J. Kim, Y. Tae, C. Park, J.-H. Choi, J. Choo, Reversible instance normalization for accurate time-series forecasting against distribution shift, in: International Conference on Learning Representations, 2021.
URL <https://openreview.net/forum?id=cGDakQo1C0p>
- [18] T. Akiba, S. Sano, T. Yanase, T. Ohta, M. Koyama, Optuna: A next-generation hyperparameter optimization framework (2019). arXiv:1907.10902.
URL <https://arxiv.org/abs/1907.10902>
- [19] A. Brusafferri, A. Ballarino, L. Grossi, F. Laurini, On-line conformalized neural networks ensembles for probabilistic forecasting of day-ahead electricity prices (2024). arXiv:2404.02722.
URL <https://arxiv.org/abs/2404.02722>
- [20] J. V. Dillon, I. Langmore, D. Tran, E. Brevdo, S. Vasudevan, D. Moore, B. Patton, A. Alemi, M. Hoffman, R. A. Saurous, Tensorflow distributions (2017). arXiv:1711.10604.
URL <https://arxiv.org/abs/1711.10604>

- [21] A. Lipiecki, B. Uniejewski, R. Weron, Postprocessing of point predictions for probabilistic forecasting of day-ahead electricity prices: The benefits of using isotonic distributional regression, *Energy Economics* 139 (2024) 107934. doi:<https://doi.org/10.1016/j.eneco.2024.107934>.
URL <https://www.sciencedirect.com/science/article/pii/S014098832400642X>
- [22] C. Guo, G. Pleiss, Y. Sun, K. Q. Weinberger, On calibration of modern neural networks, in: *Proceedings of the 34th International Conference on Machine Learning - Volume 70, ICML'17, JMLR.org*, 2017, p. 1321–1330.
- [23] A. N. Angelopoulos, E. J. Candès, R. J. Tibshirani, Conformal pid control for time series prediction, in: *Proceedings of the 37th International Conference on Neural Information Processing Systems, NIPS '23*, Curran Associates Inc., Red Hook, NY, USA, 2024.
- [24] K. C. Lichtendahl, Y. Grushka-Cockayne, R. L. Winkler, Is it better to average probabilities or quantiles?, *Management Science* 59 (7) (2013) 1594–1611. arXiv:<https://doi.org/10.1287/mnsc.1120.1667>, doi:10.1287/mnsc.1120.1667.
URL <https://doi.org/10.1287/mnsc.1120.1667>
- [25] J. Siems, K. Ditschuneit, W. Ripken, A. Lindborg, M. Schambach, J. S. Otterbach, M. Genzel, Curve your enthusiasm: concurvity regularization in differentiable generalized additive models, in: *Proceedings of the 37th International Conference on Neural Information Processing Systems, NIPS '23*, Curran Associates Inc., Red Hook, NY, USA, 2024.
- [26] X. Zhang, J. Martinelli, S. John, Challenges in interpretability of additive models, *IJCAI 2024 Workshop on Explainable Artificial Intelligence* (2024).